Entanglement Renormalization and Wavelets

Glen Evenbly and Steven R. White

Department of Physics and Astronomy, University of California, Irvine, California 92697-4575, USA
(Received 12 February 2016; revised manuscript received 11 March 2016; published 6 April 2016)

We establish a precise connection between discrete wavelet transforms and entanglement renormalization, a real-space renormalization group transformation for quantum systems on the lattice, in the context of free particle systems. Specifically, we employ Daubechies wavelets to build approximations to the ground state of the critical Ising model, then demonstrate that these states correspond to instances of the multiscale entanglement renormalization ansatz (MERA), producing the first known analytic MERA for critical systems.

In recent years tensor networks [1] have emerged as an exciting approach to both quantum mechanics and statistical mechanics that combine ideas of many-body physics with quantum information, while closely connecting simulation and analytic theory. An intriguing development within tensor networks is the multiscale entanglement renormalization ansatz (MERA) [2–4], designed to implement real-space renormalization group (RG) [5] ideas in a powerful numerical algorithm which accurately captures scale invariance and critical point behavior.

For a D-dimensional physical system, the MERA is constructed as a $(D + 1)$-dimensional tensor network, where layers in the extra dimension encode ground state correlations at different length scales. Within a numerical setting, MERA have been demonstrated [6–12] to accurately capture the critical long range behavior of lattice versions of conformal field theories (CFTs) [13,14], which are used to describe critical points. MERA also provides a framework to investigate the AdS/CFT correspondence, with the extra dimension of the MERA associated with a physical space-time dimension, making tensor networks an important topic in quantum gravity and string theory [15,16].

Wavelets and wavelet transforms (WTs) [17–21], one of the most significant developments in signal and image processing in several decades, are also closely tied to RG: ideas from RG influenced the development of wavelets, and wavelets have proved to be a useful tool in RG applications [22]. In fact, it is natural to think of compact, orthogonal WTs, such as the well-known families of WTs introduced by Daubechies [17,20], as being real-space RG transformations, but in the space of ordinary 1D functions rather than in terms of Hamiltonians or Lagrangians. Given the close connections to real-space RG of both MERA and wavelets, it is natural to ask if these two methods are connected more deeply to each other.

Here we show that this is, indeed, the case, and report on a precise relation between WTs and the MERA, that a wavelet analysis of a free particle system can be exactly mapped to a MERA. An important development results from this connection: we find the first *analytic* MERA that accurately approximates the ground state of a critical system, whereas previous constructions have always resulted from a complicated variational optimization. For the lowest order case, the two unitary gates w and u that constitute a (binary) scale-invariant MERA [4,6] can be written in a remarkably compact form,

$$w = \frac{\sqrt{3} + \sqrt{2}}{4} II + \frac{\sqrt{3} - \sqrt{2}}{4} ZZ + \frac{i(1 + \sqrt{2})}{4} XY$$
$$+ \frac{i(1 - \sqrt{2})}{4} YX$$
$$u = \frac{\sqrt{3} + 2}{4} II + \frac{\sqrt{3} - 2}{4} ZZ + \frac{i}{4} XY + \frac{i}{4} YX, \qquad (1)$$

where X, Y, Z are Pauli matrices, and where ZZ is short for $Z \otimes Z$, etc. Here unitary u is the so-called disentangler of the MERA, while w becomes the isometry of the MERA once the second input spin is fixed in the $|\uparrow\rangle$ eigenstate of Z. This MERA, which is derived using two copies of the Daubechies D4 wavelet, can be shown to approximate the ground state of the quantum critical Ising model, including the critical data of the Ising CFT. We also present a general prescription for obtaining higher order MERA and give another specific example. These analytic constructions provide an important new tool for making further progress in MERA applications, and are likely just the first example of important results from the wavelet-MERA connection.

Free fermions.—We consider the tight-binding Hamiltonian on an infinite 1D lattice of spinless fermions at half-filling,

$$H_{\text{ff}} = -\sum_r (\hat{a}_{r+1}^\dagger \hat{a}_r + \hat{a}_r^\dagger \hat{a}_{r+1}), \qquad (2)$$

with $\hat{a}$ and $\hat{a}^\dagger$ the annihilation and creation operators. In terms of the Fourier mode creation operators $\hat{b}_k^\dagger$, where k is the momentum, the ground state of H is given by occupying the negative energy modes,

$$|\psi_{\rm GS}\rangle = \prod_{|k|<\pi/2} \hat{b}_k^\dagger |0\rangle, \qquad (3)$$

while leaving positive energy modes unoccupied.

Wavelets.—We would like to use wavelets to find another set of modes $\{\hat{c}_z^{\rm Low}\}$, more localized than plane waves, but composed almost entirely of linear combinations of negative energy states, so that the ground state (GS) is approximated by filling these modes,

$$|\psi_{\rm GS}\rangle \approx \prod_z (\hat{c}_z^{\rm Low})^\dagger |0\rangle. \qquad (4)$$

Correspondingly, there will also exist a set of modes $\{\hat{c}_z^{\rm High}\}$ composed of linear combinations of positive energy states, which are unoccupied in the ground state. The accuracy of the separation into low and high energy states must be increasingly sharp as one looks more closely near the Fermi surface, which suggests we require a WT that targets the Fermi points, $\pm\pi/2$. On the other hand, standard WTs, such as Daubechies wavelets [17,18], are designed to approximately divide the Fourier components into low (scaling function) and high (wavelet) parts at each scale; see Fig. 1(a), such that they resolve degrees of freedom close to momentum $k = 0$. Thus, a direct application of known WTs is not sufficient to approximate the ground state $|\psi_{\rm GS}\rangle$. However, we will show that it is possible to combine two slightly modified Daubechies WTs to give an excellent separation of negative and positive energies, targeting $k = \pm\pi/2$.

Let us consider the Daubechies D4 wavelets (see Ref. [23], Sec. A for an introduction). We denote by $q_z(r)$ the wavelet function at scale z, and $Q_z(k)$ its (discrete) Fourier transform. At the smallest $z = 1$ scale, the D4 wavelet has support on 4 sites, where it has values $q_1 \approx [-0.483, 0.837, -0.224, -0.129]$, while wavelets at
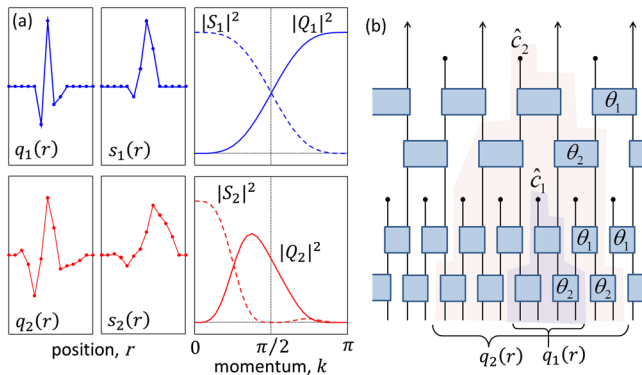
larger scales q_z, which are supported on intervals of $r = 2^{z+1} + 2^z - 2$ sites, can be easily obtained from q_1 using the cascade algorithm [21]. At level z the basis includes all translations of q_z by $d = n2^z$ sites (for integer n). The set of all wavelets—every level z, with all appropriate translations, form a complete, orthonormal basis of functions. The Daubechies wavelets are designed as high-pass filters, such that they are orthogonal to smooth functions (or, equivalently, functions that only possess low frequency components). Specifically, the D4 wavelets have two vanishing moments about $k = 0$,

$$Q_z(0) = 0, \qquad \left.\frac{\partial Q_z}{\partial k}\right|_{k=0} = 0, \qquad (5)$$

for all scales z; see also Fig. 1(a).

We now construct modified wavelets that have the vanishing moments at the Fermi points, $k \pm \pi/2$, rather than $k = 0$. We first we multiply the wavelets by a phase $\omega(r) = \exp(i\pi r)$ and then dilate by a factor of 2, but with the in-between sites set to zero:

$$\tilde{q}_z^{\rm odd}(r) = \begin{cases} (-1)^{(\frac{r+1}{2})} q_z(\frac{r+1}{2}), & r \text{ odd} \\ 0, & r \text{ even.} \end{cases} \qquad (6)$$

Similarly, we construct wavelets $\tilde{q}_z^{\rm even}$ that only have support on the even sublattice. This transformation into odd and even sublattice parts seems more natural if one considers the real linear combinations of the Fermi points $\sin(r\pi/2)$ and $\cos(r\pi/2)$, which are zero on even and odd sublattices, respectively. The key result is that the frequency space representation of these wavelets $\tilde{Q}_z^{\rm odd}(k)$ now have vanishing moments at $k = \pm\pi/2$,

$$\tilde{Q}_z^{\rm odd}\left(\pm\frac{\pi}{2}\right) = 0, \qquad \left.\frac{\partial \tilde{Q}_z^{\rm odd}}{\partial k}\right|_{\pm\frac{\pi}{2}} = 0, \qquad (7)$$

and similarly for $\tilde{Q}_z^{\rm even}$.

The modified wavelet functions are localized, in Fourier space, increasingly close to the Fermi points at larger scale z, however, they are still not sufficient to approximate the ground state $|\psi_{\rm GS}\rangle$ as they contain a mixture of negative and positive energy components. To separate the energy components, we form coherent low $l_z(r)$ and high $h_z(r)$ wavelet pairs by taking symmetric and antisymmetric combinations, respectively, of $\tilde{q}_z^{\rm odd}$ and $\tilde{q}_z^{\rm even}$,

$$l_z(r) = \tilde{q}_z^{\rm odd}(r) + \tilde{q}_z^{\rm even}(r_0 - r),$$
$$h_z(r) = \tilde{q}_z^{\rm odd}(r) - \tilde{q}_z^{\rm even}(r_0 - r). \qquad (8)$$

The constant r_0, which determines the spatial alignment of the odd and even wavelets, should be chosen in order to form wavelets with the best separation of energies; here this choice is such that the support of an even wavelet starts

FIG. 1. (a) Plots of D4 Daubechies wavelets $q_z(r)$ and scaling functions $s_z(r)$ for scales $z = 1$, 2, together with their Fourier spectra $Q_z(k)$ and $S_z(k)$. (b) The quantum circuit, built from gates $v(\theta)$ of Eq. (10) with angles $\theta_1 = \pi/12$ and $\theta_2 = -\pi/6$, implements the linear map of fermionic modes, see Eq. (12), corresponding to the D4 wavelet transform.

three sites before that of an odd wavelet it is paired with (see Ref. [23], Sec. B for details).

The symmetric and antisymmetric wavelet pairs $l_z(r)$ and $h_z(r)$, together with their frequency spectra, are plotted in Fig. 2(a) for scales $z = 1, 2$. It can be seen that they separate negative and positive energies nicely, with $l_z(r)$, to very good approximation, only containing frequencies $|k| < \pi/2$ [and vice versa for $h_z(r)$]. Thus, if we use the wavelets $l_z(r)$ and $h_z(r)$ to define a linear mapping of fermionic modes,

$$\hat{c}_z^{\mathrm{Low}} = \sum_r \hat{a}_r l_z(r),$$

$$\hat{c}_z^{\mathrm{High}} = \sum_r \hat{a}_r h_z(r), \qquad (9)$$

then the ground state $|\psi_{\mathrm{GS}}\rangle$ of the free fermion model H_{ff} can be approximated by occupying the negative energy modes $\hat{c}_z^{\mathrm{Low}}$ as per Eq. (4).

Quantum circuit.—Through Eqs. (6), (8), and (9) we have identified a discrete wavelet transform of fermionic modes that can be used to approximate the free fermion ground state. We now describe how this transform of fermionic modes can be realized as a quantum circuit, employing a formalism similar to that of Refs. [24–26], and argue that this circuit corresponds precisely to a MERA [4].
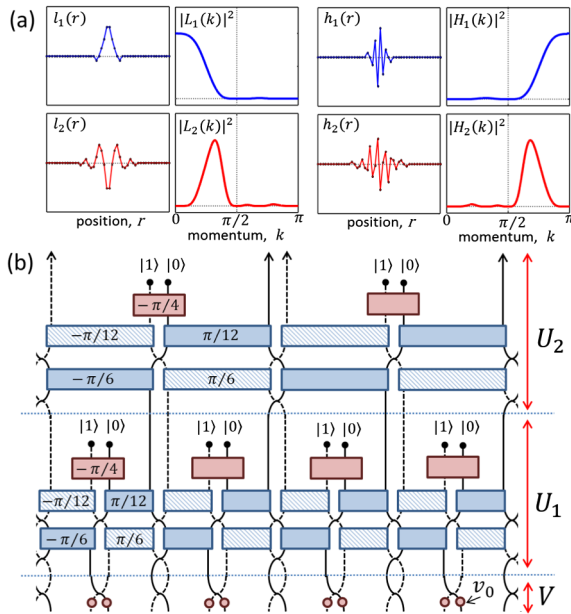

FIG. 2. (a) Plots of low frequency $l_z(r)$ and high frequency $h_z(r)$ wavelets from Eq. (8), together with their Fourier spectra $L_z(k)$ and $H_z(k)$, for scales $z = 1, 2$. (b) Quantum circuit that approximates the free fermion ground state by setting modes corresponding to low frequency l_z wavelets in the occupied $|1\rangle$ state and high frequency h_z wavelets in the unoccupied $|0\rangle$ state. The circuit is built from gates $v(\theta)$ as defined in Eq. (10) with angles θ as indicated, and v_0 represents a phase gate with angle π.

We restrict to a circuit built from two-site unitary gates v that preserve particle number

$$v_{r,r+1}(\theta) = \begin{bmatrix} 1 & 0 & 0 & 0 \\ 0 & \cos(\theta) & -\sin(\theta) & 0 \\ 0 & \sin(\theta) & \cos(\theta) & 0 \\ 0 & 0 & 0 & 1 \end{bmatrix}, \qquad (10)$$

written in the number basis $\{|00\rangle, |01\rangle, |10\rangle, |11\rangle\}$ for some angle $\theta \in [-\pi, \pi]$. It is known that unitary gates $v(\theta)$ map fermionic modes *linearly*, such that, under action of $v(\theta)$, a pair of fermionic modes $\hat{a}_r$ and $\hat{a}_{r+1}$ is mapped to a new set of modes $\hat{d}_r$ and $\hat{d}_{r+1}$,

$$\begin{bmatrix} \hat{d}_r \\ \hat{d}_{r+1} \end{bmatrix} \equiv \begin{bmatrix} \cos(\theta) & \sin(\theta) \\ -\sin(\theta) & \cos(\theta) \end{bmatrix} \begin{bmatrix} \hat{a}_r \\ \hat{a}_{r+1} \end{bmatrix}. \qquad (11)$$

Any unitary linear map on M fermionic modes can be decomposed as a product of such two-site maps, and, hence, can also be expressed as a quantum circuit built from the unitary gates $v(\theta)$ of Eq. (10). It follows that an orthogonal wavelet transform, which implements a unitary map of fermionic modes [27],

$$\hat{c}_z = \sum_r \hat{a}_r q_z(r), \qquad (12)$$

where $q_z(r)$ are the wavelet coefficients at scale z, can also be expressed as a unitary circuit built from gates $v(\theta)$. Figure 1(b) shows the circuit diagram for the D4 wavelets, which is built from two distinct unitary gates: $\{v(\pi/12), v(-\pi/6)\}$. The structure of this circuit follows from the fast wavelet transform algorithm [28], which implements the WT on 2^M sites through M recursive applications of a filter bank, and thus allows the circuit to be organized into M layers. The filter bank corresponding to a WT of $2N$ coefficients can be further decomposed into a depth N circuit of gates $\{v(\theta_1), v(\theta_2), \ldots, v(\theta_N)\}$, where the angles θ_i are fixed from the WT under consideration; see Refs. [26,29] for additional details. Notice that the circuit of Fig. 1(b) corresponding to the D4 wavelet is precisely a scale-invariant MERA. In a higher order WT, such as the D2N Daubechies wavelets with $N > 2$, the circuit would have N levels of unitary gates $v(\theta_i)$ in each layer and thus no longer correspond to a standard MERA; however, under appropriate grouping of gates, see Ref. [23] Sec. C, one could reinterpret this as a MERA of larger bond dimension.

Two copies of the circuit representation of the D4 wavelets can then be combined to construct the modified wavelet transform of Eqs. (8) and (9) that approximates the free fermion ground state, as depicted in Fig. 2(b). Here one copy of the circuit for the D4 WT is implemented on the odd sublattice, and is overlaid with a second circuit

(spatially mirrored with respect to the first) on the even sublattice. Note that the spatial mirroring is equivalent to negating the sign of the unitary angles, such that the second circuit is comprised of gates $\{v(-\pi/12), v(\pi/6)\}$. These two circuits are then coupled by $v(-\pi/4)$ gates, which generate the symmetric and antisymmetric wavelets described in Eq. (8).

The combined circuit depicted in Fig. 2(b) consists of an identical sequence of scale-invariant layers, labeled $\{U_1, U_2, \ldots\}$, but also includes an initial "transitional" layer V at the bottom. The transitional layer serves two purposes: (i) first it includes local unitary operators $v_0 = \hat{a}^\dagger \hat{a} - \hat{a}\hat{a}^\dagger$ that implement the phase change described in Eq. (6), and, (ii) second, it includes an extra set of swap gates required to give the proper wavelet alignment r_0 in Eq. (8). Under appropriate grouping of tensors, the circuit of Fig. 2(b) can be mapped to a binary MERA of bond dimension $\chi = 4$. This MERA can then be split into two copies of the $\chi = 2$ MERA from Eq. (1) for the ground state of the quantum critical Ising model, $H_{\text{Is.}} = \sum_r (-X_r X_{r+1} - Z_r)$, using known decoupling [30] and Jordan-Wigner [31] transformations, see Ref. [23], Sec. D for details.

Results and discussion.—We now analyze the accuracy of the $\chi = 2$ MERA from Eq. (1), constructed using D4 wavelets, and a $\chi = 8$ MERA, constructed using higher order wavelets (see Ref. [23], Sec. C), as approximate ground states of the quantum critical Ising model. Note that, as with the $\chi = 2$ MERA, the parameters defining the $\chi = 8$ MERA are exactly specified from a closed-form solution. The ground energy and critical data [13,14] (including central charge c, scaling dimensions Δ_i, and operator product expansion (OPE) coefficients C_{ijk}) are computed using standard MERA techniques [6–8], and the results displayed in Table I.

The wavelet-derived results reproduce the critical data of the Ising CFT, with the $\chi = 8$ MERA providing significantly better accuracy. However, we find it remarkable that the $\chi = 2$ MERA of Eq. (1) does reasonably encode the CFT, despite the simplicity of the tensors it is constructed from. A novel feature of these MERA is that some of the scaling dimensions are reproduced exactly (specifically those corresponding to primary fields $\{\mathbb{1}, \varepsilon, \psi, \bar{\psi}\}$, as well as for several of their descendants), which has never been achieved with variationally optimized MERA; see Ref. [23] Sec. F for comparison.

As usual, each layer of the MERA can be understood as implementing a step of entanglement renormalization (ER), which can be used to generate a sequence of increasingly coarse-grained Hamiltonians,

$$H_{\text{Is.}}^{[0]} \to H_{\text{Is.}}^{[1]} \to H_{\text{Is.}}^{[2]} \to H_{\text{Is.}}^{[3]} \to \ldots, \qquad (13)$$

where $H_{\text{Is.}}^{[z]}$ is the effective Hamiltonian after z steps. This RG flow is found to converge to a gapless fixed point $H_{\text{Is.}}^*$

TABLE I. Energy density, central charge c, scaling dimensions Δ_i of primary fields (and also of the Hamiltonian Δ_H), OPE coefficients C_{ijk}, of the $\chi = 2$, 8 MERA constructed using wavelets.

	Exact	MERA $\chi = 2$	MERA $\chi = 8$
Energy	$-1.27323\ldots$	-1.24212 (2.4% err.)	-1.26774 (0.4% err.)
c	0.5	0.4957	0.5041
$\Delta_{\mathbb{1}}$	0	0	0
Δ_σ	0.125	0.1402	0.1233
Δ_ε	1	1	1
Δ_μ	0.125	0.1445	0.1291
Δ_ψ	0.5	0.5	0.5
$\Delta_{\bar\psi}$	0.5	0.5	0.5
Δ_H	2	2	2
$C_{\varepsilon,\sigma,\sigma}$	0.5	0.4584	0.4957
$C_{\varepsilon,\mu,\mu}$	-0.5	-0.4201	-0.5060
$C_{\psi,\mu,\sigma}$	$\frac{e^{-i\pi/4}}{\sqrt{2}}$	$\frac{1.1422 e^{-i\pi/4}}{\sqrt{2}}$	$\frac{1.0014 e^{-i\pi/4}}{\sqrt{2}}$
$C_{\bar\psi,\mu,\sigma}$	$\frac{e^{i\pi/4}}{\sqrt{2}}$	$\frac{1.1422 e^{i\pi/4}}{\sqrt{2}}$	$\frac{1.0014 e^{i\pi/4}}{\sqrt{2}}$
$C_{\varepsilon,\psi,\bar\psi}$	i	$1.234 i$	$1.0243 i$
$C_{\varepsilon,\bar\psi,\psi}$	$-i$	$-1.234 i$	$-1.0243 i$

that approximates the thermodynamic limit of the critical Ising model; see Ref. [23], Sec. E for details. This is the first known example (analytic *or* numeric) of a critical Hamiltonian that is coarse grained to a truly gapless fixed point using ER. In previous (variational) implementations of ER, the gapless fixed point is approximated for a finite number of RG steps (which can be increased by using larger χ), before ultimately flowing to a gapped fixed point [32]. This was understood to be an inescapable consequence of finite bond dimension χ; that truncation errors introduce relevant perturbations that shift the RG flow off criticality. Here we have demonstrated that the (previously observed) inability of ER to fully reproduce a critical RG fixed point stems from a limitation of the optimization strategies used, as opposed to an inherent limitation of the finite-χ MERA.

That the RG flow from the wavelet-derived MERA converges to a gapless fixed point follows from the constraints of Eq. (7), which impose that the wavelets, corresponding to modes truncated at each RG step, have exactly vanishing component at the Fermi points, $\pm\pi/2$. This ensures that the Fermi surface remains intact under coarse graining, thus preventing a gap from opening. More generally, this result may hint towards better strategies for numerical optimization of MERA.

The wavelet methodology could be extended to allow analytic construction of MERA (and potentially branching MERA [33]) for free fermions in higher dimensions, and could also be extended to free bosonic MERA [34] which may connect with previous use of wavelets to study bosonic field theories [35]. We expect that the wavelet-MERA

relation will lead to other useful results, potentially allowing a better characterization of errors and improved implementations of MERA, and to be useful in the ongoing efforts to understand MERA in the context of AdS/CFT. Going the other way, this relation could also lead to useful advances in the design of wavelet transforms and in wavelet applications [29].

[1] J. I. Cirac and F. Verstraete, J. Phys. A **42**, 504004 (2009).

[2] G. Vidal, Phys. Rev. Lett. **99**, 220405 (2007).

[3] G. Vidal, Phys. Rev. Lett. **101**, 110501 (2008).

[4] For an introduction to ER and the MERA, see, e.g., G. Vidal, *Understanding Quantum Phase Transitions*, edited by L. D. Carr (Taylor & Francis, Boca Raton, 2010), Chap. 5; G. Evenbly and G. Vidal, Phys. Rev. B **79**, 144108 (2009).

[5] For a review of the renormalization group see, M. E. Fisher, Rev. Mod. Phys. **70**, 653 (1998).

[6] R. N. C. Pfeifer, G. Evenbly, and G. Vidal, Phys. Rev. A **79**, 040301(R) (2009).

[7] G. Evenbly, P. Corboz, and G. Vidal, Phys. Rev. B **82**, 132411 (2010).

[8] G. Evenbly and G. Vidal, Quantum criticality with the multi-scale entanglement renormalization ansatz, *Strongly Correlated Systems: Numerical Methods*, edited by A. Avella and F. Mancini, Springer Series in Solid-State Sciences (Springer, New York, 2013), Vol. 176.

[9] G. Evenbly and G. Vidal, Phys. Rev. Lett. **102**, 180406 (2009).

[10] Y.-L. Lo, Y.-D. Hsieh, C.-Y. Hou, P. Chen, and Y.-J. Kao, Phys. Rev. B **90**, 235124 (2014).

[11] G. Evenbly and G. Vidal, J. Stat. Phys. **157**, 931 (2014).

[12] J. C. Bridgeman, A. O'Brien, S. D. Bartlett, and A. C. Doherty, Phys. Rev. B **91**, 165129 (2015).

[13] P. Di Francesco, P. Mathieu, and D. Senechal, *Conformal Field Theory* (Springer, New York, 1997).

[14] M. Henkel, *Conformal Invariance and Critical Phenomena* (Springer, New York, 1999).

[15] B. Swingle, Phys. Rev. D **86**, 065007 (2012); H. Matsueda, M. Ishihara, and Y. Hashizume, Phys. Rev. D **87**, 066002 (2013); T. Hartman and J. Maldacena, J. High Energy Phys. 05 (2013) 014; A. Mollabashi, M. Nozaki, S. Ryu, and T. Takayanagi, J. High Energy Phys. 03 (2014) 098.

[16] G. Evenbly and G. Vidal, J. Stat. Phys. **145**, 891 (2011); B. Swingle, arXiv:1209.3304; X.-L. Qi, arXiv:1309.6282.

[17] I. Daubechies, Commun. Pure Appl. Math. **41**, 909 (1988).

[18] I. Daubechies, Ten Lectures on Wavelets, *CBMS Conference Series in Applied Mathematics* (SIAM, Philadelphia, 1992), Vol. 61.

[19] A. Cohen, I. Daubechies, and J. C. Feauveau, Commun. Pure Appl. Math. **45**, 485 (1992).

[20] I. Daubechies, SIAM J. Math. Anal. **24**, 499 (1993).

[21] C. S. Burrus, R. A. Gopinath, and H. Guo, *Introduction to Wavelets and Wavelet Transforms: A Primer* (Prentice-Hall, Englewood Cliffs, NJ, 1988), ISBN 0-13-489600-9.

[22] For an overview of the early connections between wavelets and RG, see G. Battle, Wavelets: A renormalization group point of view, in *Wavelets and Their Applications*, edited by M. B. Ruskai (Bartlett and Jones, Boston, 1992); G. Battle, *Wavelets and Renormalization* (World Scientific, Singapore, 1999).

[23] See Supplemental Material at http://link.aps.org/supplemental/10.1103/PhysRevLett.116.140403 for further details on (A) Daubechies wavelets, (B) achieving wavelets that separate positive and negative energies, (C) construction of higher order wavelet solutions, (D) mapping solutions to the quantum critical Ising model, (E) the RG flow of the Hamiltonian, and (F) comparison with variational MERA.

[24] G. Evenbly and G. Vidal, Phys. Rev. B **81**, 235102 (2010).

[25] A. J. Ferris, Phys. Rev. Lett. **113**, 010401 (2014).

[26] M. T. Fishman and S. R. White, Phys. Rev. B **92**, 075132 (2015).

[27] We are assuming the orthogonal wavelets are normalized to unity (under scalar product with themselves) such that they form a unitary change of basis.

[28] G. Beylkin, R. Coifman, and V. Rokhlin, Commun. Pure Appl. Math. **44**, 141 (1991).

[29] G. Evenbly and S. R. White, Representation and design of wavelets using unitary circuits (to be published).

[30] G. Evenbly and G. Vidal, Phys. Rev. Lett. **112**, 220502 (2014).

[31] J. I. Latorre, E. Rico, and G. Vidal, Quant. Inf. Comput. **4**, 48 (2004).

[32] The accuracy with which MERA approximants a scale-invariant RG flow is studied (in the related context of tensor network renormalization) in Sec. A of the Supplemental Material of: G. Evenbly and G. Vidal, Phys. Rev. Lett. **115**, 180405 (2015).

[33] G. Evenbly and G. Vidal, Phys. Rev. Lett. **112**, 240502 (2014).

[34] G. Evenbly and G. Vidal, New J. Phys. **12**, 025007 (2010).

[35] G. K. Brennen, P. Rohde, B. C. Sanders, and S. Singh, Phys. Rev. A **92**, 032315 (2015).